Diffusion of Decamethylferrocene and Decamethylferrocenium Hexafluorophosphate in Supercritical Trifluoromethane

Darío L. Goldfarb[†,‡] and Horacio R. Corti[*,†,§]

Comisión Nacional de Energía Atómica, Unidad de Actividad Química, Av. Gral. Paz 1499 (1650) San Martín, Buenos Aires, Argentina, and Departamento de Química Inorgánica, Analítica y Química Física, Facultad de Ciencias Exactas y Naturales, Universidad de Buenos Aires, Pabellón II, Ciudad Universitaria (1428) Buenos Aires, Argentina

Received: February 27, 2003; In Final Form: November 29, 2003

The diffusion coefficients of decamethylferrocene ($Fe(Cp^*)_2$) and decamethylferrocenium hexafluorophosphate ($Fe(Cp^*)_2PF_6$) in supercritical trifluoromethane (CHF_3) were measured at a temperature of 323.15 K, as a function of density, with tetrabutylammonium hexafluorophosphate ($TBAPF_6$) as the supporting electrolyte, using a voltammetric technique on a platinum microelectrode. The diffusion in subcritical CHF_3 was also studied, to analyze the differences in the behavior of both solutes in the low- and high-density regions. Application of the Oldham, Cardwell, Santos, and Bond theory allowed the effect of ion pairing on the limiting current to be considered. The density dependence of the diffusion coefficients of the different species has been discussed on the basis of the continuum hydrodynamic model and the clustering of solvent around solute molecules in the low-density supercritical region. The predictions of the compressible continuum model for the case of the diffusion of the free ions and the ion pair also have been discussed.

Introduction

Recently, the use of supercritical solvents in industrial processes such as synthesis and separation has increased remarkably.[1,2] The advantage of supercritical fluids, besides their environmentally benign characteristics, is the possibility of easily tuning their density—and, consequently, their physicochemical properties—by changing the pressure or temperature close to its critical point.[3] The properties of solutes in supercritical solvents are largely affected by density changes, and access to information on the diffusion coefficients of solutes in these media is fundamentally important, in regard to the design and efficient operation of processes that involve supercritical fluids.

The available information on the diffusion coefficient data of nonionic solutes in supercritical solvents has been summarized by Suárez et al.[4] and He.[5] Diffusion studies that use conventional techniques (the Taylor−Aris method) have been performed only in 10 supercritical solvents, and most of them correspond to supercritical CO_2, where the diffusion coefficients of more than 70 solutes have been reported. Most of the solutes studied in this solvent were aromatic hydrocarbons and long-chain ethers in the ranges of $T/T_c = 1.00-1.13$ and $\rho/\rho_c = 0.43-2.23$ (where T is the temperature, T_c the critical temperature, ρ the density, and ρ_c the critical density). In comparison, to date, only 34 solutes have been studied in the other supercritical solvents.

For ionic solutes, the studied systems are scarce. One of the techniques used in the study of ionic solutes is electrochemistry, and the results have been reviewed by Dinjus et al.[6] The first studies of electrochemical synthesis[7] used CO_2, HCl, and NH_3 as supercritical solvents; however, the results in CO_2 were discounted, because of the high resistivity[8] and because it is a poor solvent for ionic solutes, whereas corrosion problems precluded the use of HCl.

Bard and co-workers have studied several solutes using cyclic voltammetry (CV), chronoammperometry, and chronocoulometry in near-critical and supercritical NH_3,[9−11] SO_2,[12] CH_3CN,[13,14] and water[15−18] at different densities.

One should emphasize that, although water and other polar solvents have good solubility for ionic solutes in supercritical conditions, their high critical pressure (p_c) and temperature (T_c) discourage their use on industrial scales.

Wightman and co-workers[19,20] performed CV studies in supercritical CO_2 with a small amount of added water, using tetrahexylammonium hexafluorophosphate ($THAPF_6$) and tetrahexylammonium nitrate ($THANO_3$) as the supporting electrolyte. They were unsuccessful in their attempt to obtain a precise limiting current for diffusion measurements, because of the ohmic distortion of the voltammograms.

Olsen and Tallman[21,22] were the first to study diffusion in supercritical hydrofluorocarbons (HFCs). They measured the diffusion coefficients of ferrocene and cobaltocenium hexafluorophosphate in chlorodifluoromethane (critical dielectric constant of $\epsilon_c = 2.31$, $T_c = 369.2$ K, and $p_c = 4.97$ MPa), using tetrabutylammonium tetrafluoroborate ($TBABF_4$) as the supporting electrolyte, at densities of $0.81-1.02$ g/cm^3.

Abbott and co-workers[23−25] have also performed electrochemical measurements in supercritical CO_2, 1,1,1,2-tetrafluoroethane ($\epsilon_c = 3.5$), and difluoromethane ($\epsilon_c = 4.9$); however, these studies were restricted to electrical conductivity and faraday efficiency measurements.

In the accompanying article,[26] we performed a precise and comprehensive study of the electrical conductivities of decamethylferrocenium hexafluorophosphate ($Fe(Cp^*)_2PF_6$) and tetrabutylammonium hexafluorophosphate ($TBAPF_6$) in supercritical trifluoromethane (CHF_3) ($T_c = 299.3$ K, $p_c = 4.858$ MPa,

* Author to whom correspondence should be addressed. E-mail address: hrcorti@cnea.gov.ar.

† Comisión Nacional de Energía Atómica.

‡ Present address: Advanced Lithography Materials and Processes, IBM Thomas J. Watson Research Center, P.O. Box 218, Yorktown Heights, NY 10598.

§ Universidad de Buenos Aires.

10.1021/jp034511u CCC: $27.50
Published on Web 02/17/2004

$\rho_c = 0.529$ g/cm^3) at a temperature of 323.15 K, over a wide range of densities. The main objective of the electrical conductivity study was to analyze the validity of the incompressible continuum model and the compressible continuum model (CC model) that was developed for supercritical fluids[27] in low-permittivity supercritical CHF_3, based on the behavior of the molar conductivity at infinite dilution.

Our analysis of the limiting molar conductivity, as a function of the density, indicated that a simple continuum model such as that expressed by Walden's rule is not valid in supercritical CHF_3. On the other hand, the CC model, based on the electrostriction effect on the local density and the local viscosity around the ions, describes the limiting conductivity for $TBAPF_6$ rather well, whereas, for $Fe(Cp^*)_2PF_6$, the predictions of the CC model are consistent with the experimental data at densities of >0.7 g/cm^3 but overestimate the limiting conductivity below that density. The CC model predicts limiting conductivities that are similar to the experimental values in the low-density region if the solvation radius of the cation increases as the density decreases.

This observation is consistent with the presence of large local solvent density fluctuations around the ions, mainly in the low-density region, which increases the ion friction, in comparison to normal solvents. These findings, along with preliminary results[28] of voltammetric measurements of the limiting current on microelectrodes for the oxidation of decamethylferrocene ($Fe(Cp^*)_2$) and the reduction of decamethylferrocenium ($Fe(Cp^*)_2^+$) in supercritical CHF_3, using $TBAPF_6$ as the supporting electrolyte, encouraged us to use CHF_3 as a model supercritical fluid for a systematic study of the transport properties of ionic and neutral solutes.

The diffusion study performed in this article shares the same objective with the electrical conductivity study, and its purpose is to confirm the failure of the simple incompressible continuum model to describe the diffusion of electrolytes in low-temperature supercritical fluids and test the validity of the CC model on the density range studied. It also analyzes the differences between the diffusion behavior of electrolytes (free ions and ion pairs) and nonelectrolytes.

The trace diffusion coefficient (D_i) of the ions and the molar conductivity at infinite dilution (λ°_i) are related in a simple way by the well-known Nernst−Einstein relationship:

$$D_i = \frac{k_B T}{zeF}\lambda^\circ_i \qquad (1)$$

where k_B is the Boltzmann constant, F the Faraday constant, and ze the charge of the ions. Therefore, the measurement of the diffusion coefficient of the electrolyte yields information on a transport process that is directly related to that obtained by measuring electrical conductivity, provided that the species that participate in both processes are the same (free ions and ion pairs).

In this work, we determine the diffusion coefficients of $Fe(Cp^*)_2$ and $Fe(Cp^*)_2PF_6$ in subcritical and supercritical CHF_3 at 323.15 K over a wide range of densities by measuring the limiting voltammetric currents on microelectrodes, under the condition that the current is difusionally controlled. The main difference with the AC electrical conductivity technique that was used in the previous article[26] is that both the neutral solute ($Fe(Cp^*)_2$) and the ion pairs of the $Fe(Cp^*)_2PF_6$ salt make an important contribution to the diffusional current, and it is possible to obtain information on the mobility of these species, which does not contribute to the electrical conductivity. Thus, the voltammetric technique will allow us to complete the study of one of the systems studied by electrical conductivity, obtaining information on the density dependence of the diffusion coefficients and comparing it with that obtained for the electrical mobility.

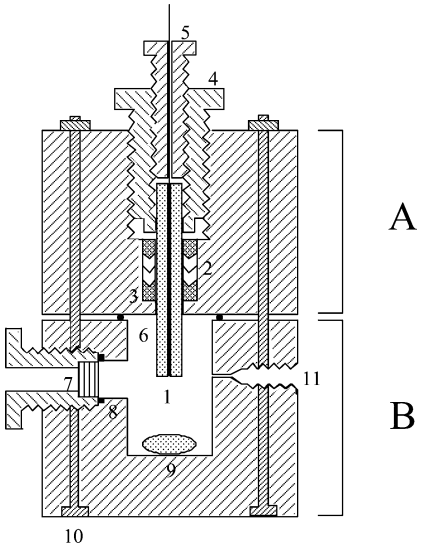

Figure 1. Schematic diagram of the high-pressure electrochemical cell (see text for references).

Experimental Section

The voltammetric technique on disk microelectrodes that were used to study the oxidation of $Fe(Cp^*)_2$ and the reduction of decamethylferrocenium ($Fe(Cp^*)_2^+$) in supercritical CHF_3 with $TBAPF_6$ as the supporting electrolyte[28] was extended in this work to a wider range of solvent densities and concentrations of the support and electroactive electrolytes.

The very small diffusional currents obtained on microelectrodes and the low solubility of the solutes restricted our density range to $\rho > 0.497$ g/cm^3. Nevertheless, the analysis of the diffusion coefficients can be done over the entire density range studied, whereas, in the case of the limiting electrical conductivity, the analysis is restricted to $\rho > 0.6$ g/cm^3.

The disk microelectrode was a 25-μm-diameter platinum wire (Goodfellow) that was sealed in a glass tube (6 mm outside diameter, 1 mm inside diameter) mounted in a high-pressure electrochemical cell, shown in Figure 1. The cell was built of titanium and the upper block (A) contains the working microelectrode (labeled as "1" in Figure 1). The pressure seal is accomplished by compressing polytetrafluoroethylene (PTFE) chevron gaskets (labeled as "2") and titanium gaskets (labeled as "3") against the glass tubing. A compression nut (labeled as "4") and a safety bolt (labeled as "5") completed the pressure seal on the microelectrode. A 1-mm-diameter silver wire (Goodfellow) that was wrapped around the working electrode (not shown in Figure 1) was used as a pseudo-reference electrode, whereas the entire body of the cell acted as a counter electrode.

The lower block (B) contains two 15-mm-diameter sapphire windows (labeled as "7") with PTFE O-rings (labeled as "8") as pressure seals that allow visual inspection of the interior of the electrochemical cell. The cell parts are held together by five stainless-steel bolts (labeled as "10"), with a gold O-ring (labeled as "6") 3 mm in diameter and 0.5 mm thick that acted as a pressure seal. The total volume of the electrochemical chamber is 9.26 cm^3, as determined using a high-pressure volumetric technique.

The loading procedure is as follows. The solute that is dissolved in dichloromethane is charged into the cell by means

of a syringe, and then the solvent is evaporated under vacuum. CHF_3 from the storage cylinder is loaded into a high-pressure manual pump and then transferred into the cell through one of the input ports (labeled as "11" in Figure 1). High-performance liquid chromatography (HPLC) tubing with an external diameter of $^1/_{16}$ in. (PEEK) was used to deliver the pressurized fluid into the chamber. The solution inside the cell was stirred by means of a magnetic bar (labeled as "9"). Pressure was measured with a pressure transducer (Burster, pressure range of 0−200 bar, with an accuracy of 0.05 bar). Temperature control on the high-pressure chamber was achieved by surrounding the cell with coiled copper tubing. Water was recirculated and thermostatized using a temperature controller (Thermomix). The high-pressure chamber and the copper coil were thermally insulated using a Styrofoam material. An electrically insulated thermocouple wire inserted through one of the high-pressure inlet ports that was used to read the temperature inside the cell to within 0.1 K. The complete high-pressure system was enclosed in a Faraday cage during the measurements, to minimize the presence of inductively coupled electrical noise during the current measurements.

A potentiostat (Oxford Instruments) that was designed to measure the currents in the 10^{-12} A range (and was connected to a personal computer (PC) through a IEEE-488 interface) was used to apply the voltage signal and measure the current.

Trifluoromethane (>99% CHF_3, K. H. Muller Laboratories) was dried over potassium hydroxide (KOH) that was contained in a stainless-steel cylinder, to eliminate traces of water. $TBAPF_6$ and $Fe(Cp^*)_2$ (Fluka, electrochemical grade) were used as-received. $Fe(Cp^*)_2PF_6$ was synthesized and purified following a procedure described in the literature.[29] The solid was dried at 110 °C for 12 h and was used without recrystallization. All solids were stored in a vacuum desiccator prior to their use.

Theoretical Background

The determination of the diffusion coefficients from the limiting voltammetric currents measured in systems with strong ion association, such as those observed in low-dielectric-constant supercritical fluids, requires a theory to assess the effect of ionic association on the current. Several approaches to address the electron-transfer process on microelectrodes are found in the literature,[30−35] including the formation of ion pairs of both the electroactive species and the supporting electrolyte.

In this work, a theory developed by Oldham, Cardwell, Santos, and Bond[36] (OCSB theory) will be applied. The success of the OCSB theory to describe accurately the contribution of migrational processes to the overall faradaic current when variable quantities of supporting electrolyte are added to the solution was demonstrated in a previous study of the reduction of the decamethylferrocenium ion ($Fe(Cp^*)_2^+$) in dichloromethane at microelectrodes.[37] In that work, the limiting current, as measured with variable amounts of $TBAPF_6$ as the supporting electrolyte, was used to calculate the diffusion coefficient of the $Fe(Cp^*)_2^+$ ion and its ion pair with the hexafluorophosphate anion.

The species considered by the OCSB theory are shown in Table 1 for the particular system studied in this work. The theory[36] accounts for the steady-state one-electron process reduction of the $Fe(Cp^*)_2^+$ ion and its ion pair with the supporting anion:

$$Fe(Cp^*)_2^+(soln) + e \rightarrow Fe(Cp^*)_2(soln)$$

$$Fe(Cp^*)_2PF_6(soln) + e \rightarrow PF_6^-(soln) + Fe(Cp^*)_2(soln)$$

TABLE 1: Species Considered in the Reduction of $Fe(Cp^*)_2PF_6$ with $TBAPF_6$ as the Supporting Electrolyte

species	role	i	z_i	ν_i
$Fe(Cp^*)_2^+$	electroactive cation	1	1	$1-f$
$(Fe(Cp^*)_2^+ PF_6^-)$	electroactive ion pair	2	0	f
PF_6^-	anion (common)	3	−1	$-f$
$TBAPF_6$	supporting ion pair	4	0	0
TBA^+	supporting cation	5	1	0

Because the ion-pair/free-ion equilibrium is assumed to occur instantaneously at all points in the system, we can consider the ion pair to be electroactive, even when the $Fe(Cp^*)_2^+$ ion is the only free electroactive species.

The theory considers the ion-pair formation of the electroactive cation with the common PF_6^- anion and the pair formation of the supporting electrolyte through the equilibria

$$PF_6^-(soln) + Fe(Cp^*)_2^+(soln) \leftrightarrow Fe(Cp^*)_2PF_6(soln)$$

$$PF_6^-(soln) + TBA^+(soln) \leftrightarrow TBAPF_6(soln)$$

characterized by the equilibrium quotients (see Table 1 for subindexes):

$$\beta_2 = \frac{c_2}{c_1 c_3} \tag{2}$$

and

$$\beta_4 = \frac{c_4}{c_3 c_5} \tag{3}$$

The concentrations of the five species could be obtained by solving eqs 2 and 3, along with the conservation equation for an electrode of radius r:

$$0 = \frac{\nu_i I_L}{F} + G_i + 2\pi r^2 D_i\left[\frac{\partial c_i}{\partial r} + z_i c_i\left(\frac{F}{RT}\right)\left(\frac{\partial \phi}{\partial r}\right)\right] \tag{4}$$

the material balances in the bulk solution,

$$c_1^b + c_2^b = c_E \tag{5}$$

$$c_4^b + c_5^b = c_S \tag{6}$$

$$c_2^b + c_3^b + c_4^b = c_S + c_E \tag{7}$$

(where c_E and c_S represent the analytical concentrations of the salt that contains the electroactive species and the supporting electrolyte, respectively), and the boundary conditions on the electrode surface,

$$c_1^s = c_2^s = 0 \tag{8}$$

$$c_3^s = c_5^s \tag{9}$$

The first term in eq 4 represents the creation (or depletion) of the species i for the electrode reaction, where I_L is the limiting current. G_i is the concentration change rate of species i by ion association, and the third term combines the concentration change by diffusion and migration at a radial distance r from the electrode (F is the Faraday constant and ϕ is the local electrical potential).

The conservation equation has no analytical solution; however, it is possible to find a numerical algorithm to calculate I_L in terms of the analytical concentrations c_E and c_S, the

equilibrium quotients β_2 and β_4, and the four diffusion coefficients ratios D_i/D_1 (where $i = 2, 3, 4, 5$).

An important parameter of the OCSB theory is the support ratio (SR), which is defined as[35]

$$SR = \frac{c_S}{c_E} \tag{10}$$

because it determines the magnitude of I_L. Thus, for instance, in the case where all the diffusion coefficients are equal and $\beta_2 \leq \beta_4$, the I_L value in the absence of a supporting electrolyte ($SR \rightarrow 0$) is twice the value in an excess of supporting electrolyte ($SR \rightarrow \infty$). On the other hand, the lower the association of the supporting electrolyte, the smaller the concentration of the former to eliminate the migrational component.

For several particular cases,[36] the value of I_L can be obtained explicitly. Thus, for a disk microelectrode of radius r, which is the geometry used in this work, we have the following expressions for I_L.

No Supporting Electrolyte (SR = 0). For the case where no supporting electrolyte is present,

$$\frac{I_L}{8FrD_1c_E} = \frac{D_2}{D_{13}} + \left(1 - \frac{D_2}{D_{13}}\right)\frac{(1 + 4\beta_2 c_E)^{1/2} - 1}{2\beta_2 c_E} \tag{11}$$

where $2/D_{13} = (1/D_1) + (1/D_3)$.

In this case, I_L is dependent on the diffusivities of the three electroactives species and the ion-pair formation constant of the electroactive cation. In eq 11, one can distinguish a case of strong association ($\beta_2 c_E > 100$):

$$I_L = 8FD_2\left(\frac{1}{2} + \frac{D_1}{2D_3}\right)c_E r \tag{12}$$

where I_L is determined mainly by the ion pair, from the weak association case ($\beta_2 c_E < 1$):

$$I_L = 8FD_1c_E r \tag{13}$$

where I_L is dominated by the electroactive cation.

Excess of Supporting Electrolyte ($c_S > c_E$). For the case where there is an excess of supporting electrolyte:

$$I_L = 4FD_2c_E r \tag{14}$$

In this case, the electroactive species is ion-paired and transport is purely diffusive. Note that, in eq 14, I_L is related to the diffusivity of the ion pair, and the greater the value of β_2, the lower the concentration of supporting electrolyte (c_S) that is necessary to reach this limit.

The previously available tests for the OCSB theory are restricted to low-dielectric-constant organic solvents.[37,38] In this work, we will apply, for the first time, the OCSB theory to the calculation of diffusion coefficients in supercritical fluids.

Results and Discussion

The properties of pure CHF_3 on the range of pressure studied in this work are available from the literature[39−41] and were reported elsewhere.[26,28] In a previous study[26] of this system, we reported the electrical conductivity of $Fe(Cp^*)_2PF_6$ and $TBAPF_6$ in supercritical CHF_3 at 323.15 K, as a function of salt concentration at several densities. From these data, we were able to obtain the association constants of both salts (β_2 and β_4, using the nomenclature previously defined) over the entire range of densities that are of interest to this work.

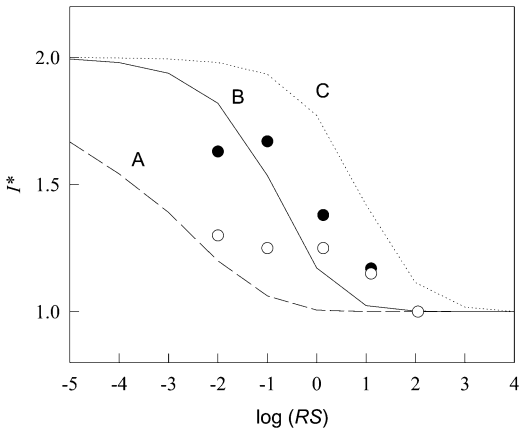

Figure 2. Limit current (I^*), as a function of the support ratio (SR), for the reduction of $Fe(Cp^*)_2PF_6$ in supercritical CHF_3 at 323.15 K with $TBAPF_6$ as the supporting electrolyte at (●) $\rho = 0.65$ g/cm^3 and (○) $\rho = 0.85$ g/cm^3, compared to the values predicted by OCSB theory for $\beta_2 c_E = 100$ and $\beta_4 c_E = 1$ (curve A), $\beta_2 c_E = 1$ and $\beta_4 c_E = 1$ (curve B), and $\beta_2 c_E = 1$ and $\beta_4 c_E = 100$ (curve C). For calculation purposes, the diffusion coefficients for all free and associated species are assumed to be equal. Analytical concentrations for all species are shown in Table 2.

TABLE 2: Limiting Current (I_L) for the Reduction of $Fe(Cp^*)_2PF_6$ in Supercritical CHF_3 at 323.15 K at Different Densities (ρ)

concentration (mol dm^{-3})		support ratio,		I_L^{norm}	
c_S	c_E	SR	I_L (nA)	(nA mol dm^{-3})	I^*
		$\rho = 0.65$ g/cm^3			
5.1×10^{-4}	5.0×10^{-6}	1.02×10^{2}	0.24	4.8×10^{4}	1.00
5.15×10^{-4}	5.0×10^{-5}	1.03×10^{1}	2.8	5.6×10^{4}	1.17
5.25×10^{-5}	5.0×10^{-5}	1.05×10^{0}	3.3	6.6×10^{4}	1.38
5.0×10^{-6}	5.1×10^{-5}	9.8×10^{-2}	4.1	8.0×10^{4}	1.67
5.0×10^{-7}	5.0×10^{-5}	1.0×10^{-2}	3.9	7.8×10^{4}	1.63
		$\rho = 0.85$ g/cm^3			
5.1×10^{-4}	5.0×10^{-6}	1.02×10^{2}	0.15	3.0×10^{4}	1.00
5.15×10^{-4}	5.0×10^{-5}	1.03×10^{1}	1.75	3.5×10^{4}	1.15
5.25×10^{-5}	5.0×10^{-5}	1.05×10^{0}	2.0	4.0×10^{4}	1.25
5.0×10^{-6}	5.1×10^{-5}	9.8×10^{-2}	1.9	3.7×10^{4}	1.25
5.0×10^{-7}	5.0×10^{-5}	1.0×10^{-2}	1.9	3.8×10^{4}	1.30

Table 2 shows the voltammetric limiting current for the reduction of $Fe(Cp^*)_2PF_6$ in supercritical CHF_3 at 323.15 K and densities of 0.65 and 0.85 g/cm^3 at different concentrations of supporting electrolyte. As expected, according to the OCSB theory, the reduction of the $Fe(Cp^*)_2^+$ cation is strongly influenced by the concentration of supporting electrolyte (c_S).

The results in Table 2 are expressed in terms of the normalized current $I_l^{norm} = I_l/c_E$, to eliminate the effect of the electroactive ion concentration and the reduced current I^*, which is defined by the relation

$$I^* = \frac{I_l^{norm}(SR)}{I_l^{norm}(SR \rightarrow \infty)} \tag{15}$$

In Figure 2, we compare our results with those calculated for fixed values of the ion-pair formation constants and diffusion coefficients. It is clear that the qualitative behavior predicted by the OCSB theory is observed; the decrease in the concentration of supporting electrolyte increases the value of I_L, because of the increases in the migration current.

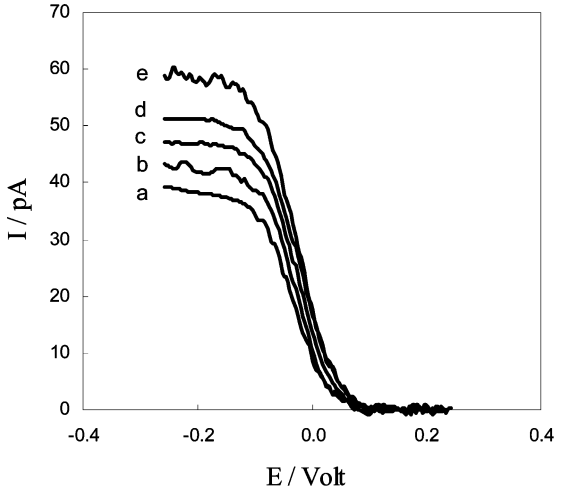

Figure 3. Linear sweep voltammograms of $Fe(Cp^*)_2PF_6$ in supercritical CHF_3 at 323.15 K and densities of $\rho = 0.9058$ g/cm^3 (curve a), $\rho = 0.8051$ g/cm^3 (curve b), $\rho = 0.7080$ g/cm^3 (curve c), $\rho = 0.6025$ g/cm^3 (curve d), and $\rho = 0.4971$ g/cm^3 (curve e). Scan rate was 5 mV/s.

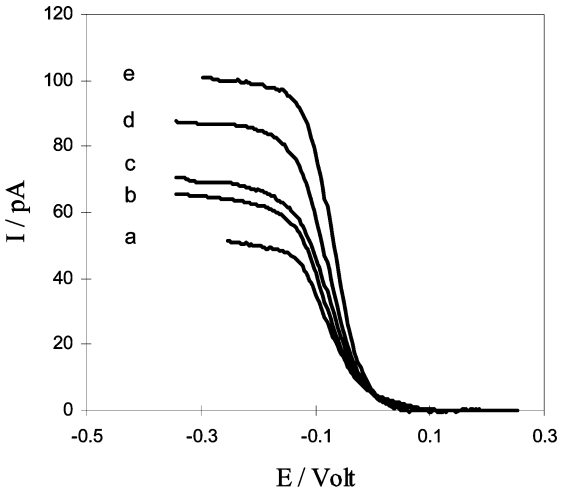

Figure 4. Linear sweep voltammograms of $Fe(Cp^*)_2PF_6$ in subcritical CHF_3 at several temperatures and pressures: 261.1 K and 179.6 bar (curve a), 261.1 K and 51.2 bar (curve b), 282.5 K and 178.7 bar (curve c), 292.6 K and 114.8 bar (curve d), and 282.5 K and 60.6 bar (curve e). Scan rate was 5 mV/s.

The ion-pair formation constant β_2, measured in supercritical CHF_3,[26] ranged from 6.6×10^4 dm^3 mol^{-1} ($\rho = 0.90$ g/cm^3) to 1.2×10^6 dm^3 mol^{-1} ($\rho = 0.65$ g/cm^3), which was indicative that the ion pair of $Fe(Cp^*)_2PF_6$ is the predominant species in this system. To determine the diffusion coefficient of the ion pair, we performed steady-state voltammetric experiments in supercritical CHF_3 with an excess of supporting electrolyte (SR = 100), in such a way that eq 14 can be used to calculate D_2. The results of these voltammograms are shown in Figure 3.

The same procedure was used to obtain the diffusion coefficient D_2 in subcritical CHF_3, and the corresponding voltamograms are shown in Figure 4 for several temperatures and pressures. Table 3 summarizes the measured I_L values and the calculated D_2 values, along with the reported values of density[39] and viscosity[40] that will be used later to analyze the diffusion process over the entire density range.

$Fe(Cp^*)_2$ was also studied using the high-pressure electrochemical cell. In this case, the oxidation product is the $Fe(Cp^*)_2^+$ ion and the voltammograms obtained in supercritical and subcritical CHF_3 in an excess of $TBAPF_6$ are shown in Figures 5 and 6, respectively. The oxidation of $Fe(Cp^*)_2$ proceeds reversibly, and the ohmic drop (IR) increases as the density decreases.[28] The results for the oxidation of $Fe(Cp^*)_2$ are listed in Table 4, where we have let D_0 represent the diffusion coefficient of $Fe(Cp^*)_2$.

TABLE 3: Limiting Currents (I_L) and Diffusion Coefficients of $Fe(Cp^*)_2PF_6$ (D_2) in Supercritical (323.15 K) and Subcritical CHF_3 with $TBAPF_6$ (Support Ratio of SR = 100) at Several Concentrations, as a Function of Density

pressure, p (bar)	density, ρ (g/cm^3)	viscosity, η (10^{-5} Pa s)	I_L (pA)	D_2 (10^{-5} cm^2/s)
	$T = 323.15$ K, $c_E = 1.55 \times 10^{-6}$ mol dm^{-3}			
103.88	0.7501	5.14	54	7.3
115.76	0.8011	5.66	51	6.9
132.37	0.8519	6.22	51	6.9
132.37	0.8519	6.22	49	6.6
156.97	0.9052	6.87	47	6.2
	$T = 323.15$ K, $c_E = 1.01 \times 10^{-6}$ mol dm^{-3}			
76.66	0.4971	3.23	60	12.3
76.66	0.4971	3.23	57	11.7
76.66	0.4971	3.23	52	10.7
80.64	0.5533	3.58	56	11.5
80.64	0.5533	3.58	52	10.6
84.61	0.6025	3.91	51	10.5
84.61	0.6025	3.91	48	9.8
88.74	0.6454	4.23	48	9.9
96.65	0.7080	4.75	45	9.2
104.60	0.7537	5.18	42	8.7
116.88	0.8051	5.70	39	8.1
132.21	0.8515	6.21	39	8.0
157.33	0.9058	6.88	35	7.1
	$T = 323.15$ K, $c_E = 4.99 \times 10^{-6}$ mol dm^{-3}			
88.70	0.6450	4.23	222	9.2
88.70	0.6450	4.23	229	9.5
96.53	0.7072	4.75	214	8.9
96.53	0.7072	4.75	209	8.7
104.64	0.7539	5.18	195	8.1
116.40	0.8034	5.68	193	8.0
132.21	0.8515	6.21	156	6.5
157.25	0.9056	6.87	156	6.5
	$T = 292.87$ K, $c_E = 3.50 \times 10^{-6}$ mol dm^{-3}			
60.57		6.99	91	5.4
65.27		7.22	84	5.0
74.28		7.64	86	5.1
94.82		8.50	76	4.5
114.77		9.21	74	4.4
148.86		10.2	68	4.0
	$T = 282.45$ K, $c_E = 4.64 \times 10^{-6}$ mol dm^{-3}			
60.61		8.80	95	4.3
96.93		10.1	68	3.1
115.6		10.6	66	2.9
178.71		12.0	66	2.9
	$T = 261.06$ K, $c_E = 4.64 \times 10^{-6}$ mol dm^{-3}			
51.23		12.3	63	2.8
101.85		13.3	60	2.7
179.58		14.9	47	2.1

Several theoretical and semiempirical correlations have been proposed to describe the behavior of solute trace diffusion coefficients in supercritical solvents.[4] One of the theoretical relationships that is valid in the continuum solvent regime (normal dense liquids) is the Stokes−Einstein equation:

$$D = \frac{k_B T}{AR\eta} \tag{16}$$

where R is the solute radius, η the viscosity of the medium, and A a constant that is dependent on the friction condition ($A = 6\pi$ for stick and $A = 4\pi$ for slip) of the solute in the continuum solvent.

The Stokes−Einstein (SE) correlation indicates that a plot of D/T vs $1/\eta$ should be linear, provided that the continuum

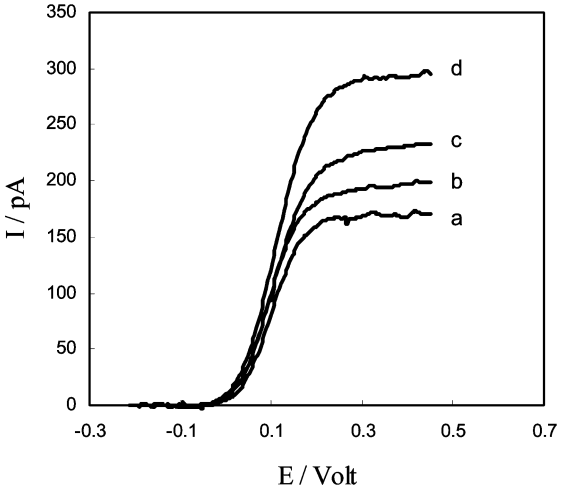

Figure 5. Linear sweep voltammograms of $Fe(Cp^*)_2$ in supercritical CHF_3 at 323.15 K and densities of $\rho = 0.9045$ g/cm^3 (curve a), $\rho = 0.8043$ g/cm^3 (curve b), $\rho = 0.7075$ g/cm^3 (curve c), and $\rho = 0.6011$ g/cm^3 (curve d). Scan rate was 5 mV/s.

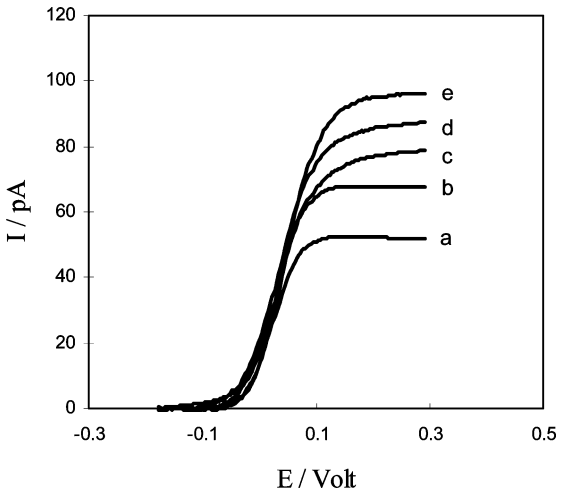

Figure 6. Linear sweep voltammograms of $Fe(Cp^*)_2$ in subcritical CHF_3 at several temperatures and pressures: 261.9 K and 82.1 bar (curve a), 282.4 K and 179.1 bar (curve b), 292.31 K and 149.8 bar (curve c), 292.31 K and 94.4 bar (curve d), and 292.31 K and 70.5 bar (curve e). Scan rate was 5 mV/s.

hydrodynamic regime is valid for the solute considered. For instance, that is the case for the diffusion of diethyl ether in supercritical CO_2,[42] where the SE correlation is valid over the entire range of reduced densities ($0.8 < \rho/\rho_c < 2.3$). However, in other systems that have been studied, the SE correlation breaks at a reduced density of 1.4−1.7, as is the case of the diffusion of benzene and naphthalene in supercritical CO_2.[43−46]

Hayduk and Cheng[47] proposed a modified version of the SE equation for the low-density region:

$$D = C\left(\frac{T}{\eta}\right)^{\beta} \qquad (17)$$

where C and β are constants ($\beta < 1$). Debenedetti and Reid[48] determined that the diffusion of benzoic acid in supercritical SF_6 follows this empirical expression, and they noted that the breaking point where diffusion goes from a hydrodynamic limit valid in the high-density region to the low-density regime has not been explained yet from first principles.

Summarizing, the SE correlation, when applied to the diffusion of solutes in supercritical fluids, has a tendency to overestimate the diffusion coefficient in the low-density region; this fact has sometimes been ascribed to experimental errors.[49]

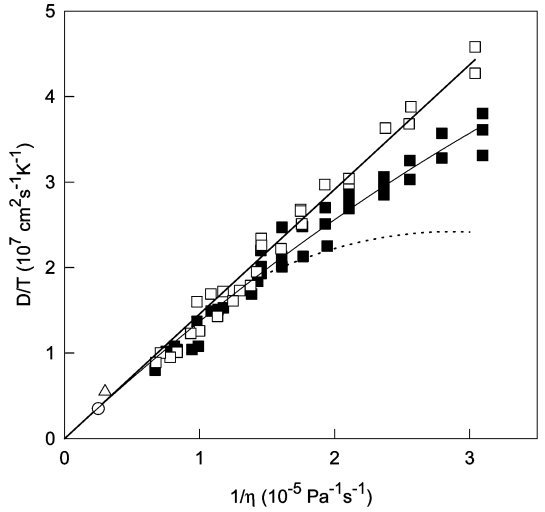

Figure 7. Stokes−Einstein plots for (■) $Fe(Cp^*)_2PF_6$ and (□) $Fe(Cp^*)_2$ in CHF_3, as well as for $Fe(Cp^*)_2PF_6$ in (○) dichloromethane and (△) acetonitrile. Dashed line corresponds to the calculated values with the CC model (see text).

TABLE 4: Limiting Currents (I_L) and Diffusion Coefficients of $Fe(Cp^*)_2$ in Supercritical (323.15 K) and Subcritical CHF_3 with $TBAPF_6$ (Support Ratio of SR = 100) at Several Concentrations, as a Function of Density

pressure, p (bar)	density, ρ (g/cm^3)	viscosity, η (10^{-5} Pa s)	I_L (pA)	D_0 (10^{-5} cm^2/s)
$T = 323.15$ K, $c_E = 1.23 \times 10^{-6}$ mol dm^{-3} (SR = 0)				
77.38	0.5076	3.29	82	13.8
77.38	0.5076	3.29	88	14.8
84.69	0.6034	3.92	71	11.9
96.61	0.7078	4.75	57	9.6
117.35	0.8068	5.72	51	8.7
117.35	0.8068	5.72	51	8.6
156.85	0.9049	6.87	44	7.4
156.85	0.9049	6.87	45	7.6
$T = 323.15$ K, $c_E = 4.83 \times 10^{-6}$ mol dm^{-3}				
84.49	0.6011	3.90	292	13.0
88.42	0.6424	4.21	273	12.0
96.57	0.7075	4.75	229	9.8
104.80	0.7547	5.19	224	9.6
116.64	0.8043	5.69	189	8.1
133.09	0.8538	6.24	167	7.2
156.61	0.9045	6.86	171	7.3
$T = 292.3$ K, $c_E = 3.50 \times 10^{-6}$ mol dm^{-3}				
60.45		7.03	96	5.7
65.26		7.26	88	5.2
74.95		7.71	85	5.1
94.42		8.52	85	5.0
114.33		9.23	84	5.0
149.78		10.2	79	4.7
$T = 282.4$ K, $c_E = 4.34 \times 10^{-6}$ mol dm^{-3}				
42.73		8.02	95	4.6
60.61		8.83	85	4.1
96.93		10.0	74	3.6
115.60		10.7	73	3.5
178.71		12.0	60	2.9
$T = 261.9$ K, $c_E = 4.34 \times 10^{-6}$ mol dm^{-3}				
82.07		12.8	52	2.5
142.23		14.1	55	2.6
178.83		14.8	49	2.3

The SE correlation plot for the diffusion coefficients of the $Fe(Cp^*)_2PF_6$ ion pair and the neutral $Fe(Cp^*)_2$ in CHF_3 is shown in Figure 7. The plot includes the high-density region that corresponds to the normal liquid CHF_3, and, for completeness,

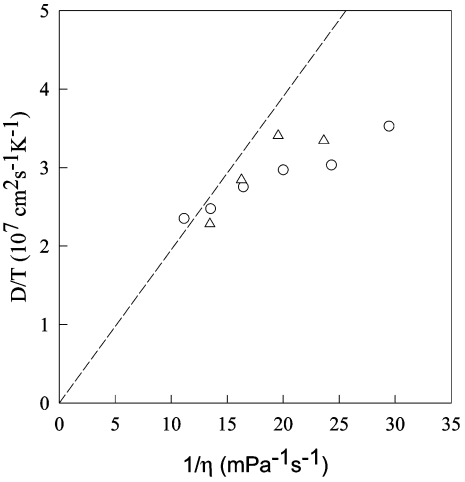

Figure 8. Stokes−Einstein correlation for the diffusion of 6-nitro-BIPS in (△) CO_2 and (○) CHF_3.

we have added diffusion coefficients for $Fe(Cp^*)_2PF_6$ that have been measured in organic solvents at 298.15 K.[37,50]

For the neutral $Fe(Cp^*)_2$, the SE correlation is valid over the entire viscosity range studied (0.033−0.149 mPa s), and the hydrodynamic radius obtained from eq 15 with stick conditions is $r = 0.503$ nm. In the case of the $Fe(Cp^*)_2PF_6$ ion pair, the SE correlation is valid in the dense region ($\eta > 0.070$ mPa s), with an effective radius of $R = 0.574$ nm. At lower densities (viscosities), the measured diffusion coefficients lie below the SE predictions, which indicates that r increases as ρ decreases.

This behavior is consistent with that observed[26] for the molar conductivity at infinite dilution of $Fe(Cp^*)_2PF_6$ in the same density region ($\rho < 0.7$ g/cm^3), and it is related to the local solvent density increase around the ion pair. The dipolar nature of the ion pair seems to be effective for the clustering of solvent molecules; however, this is not possible in the case of the $Fe(Cp^*)_2$ molecules.

Similar behavior is observed in Figure 8 for the diffusion coefficient of the polar (merocianine) form of 6-nitro-BIPS (1′,3′,3′-trimethyl-6-nitrospiro[2H-1-benzopyran-]2,2′-indoline) in supercritical CHF_3 and CO_2, as measured by Kanda et al.,[51] using a transient grating technique. In the merocianine isomer form, there is charge separation and the clustering of solvent creates a deviation from the SE correlation in the same viscosity region observed in this work.

To assess the magnitude of the local solvent density increase in the low-density region, we calculated the difference between the bulk viscosity plotted in Figure 7 and the *local viscosity*, which is obtained by extrapolating the viscosity on the SE line for each value of D/T. The resulting values of $\Delta\eta$ were then converted to $\Delta\rho$ values ($\Delta\rho = \rho_{local} - \rho_{bulk}$) using the viscosity data as a function of density.[40] Figure 9 shows the results obtained for reduced densities in the range of 0.94−1.71. The excess of solvent density is less than that found in supercritical CO_2;[52,53] however, note that our study involves the region close to and above the critical density ρ_c, and the extension of the local density excess is known[54] to be a maximum at $\rho < \rho_c$.

It is worthwhile to compare the excess of solvent density obtained for $Fe(Cp^*)_2PF_6$ in supercritical CHF_3 at 323.15 K with that predicted by the CC model.[27] The CC model was developed to explain the increase in local density around the ions that is due to solvent electrostriction. In this case, we have an ion pair—that is, two opposite charges separated by a distance equal to the effective radius of the ion pair. If we assume that the solvent electrostriction on the ion pair is equivalent to that

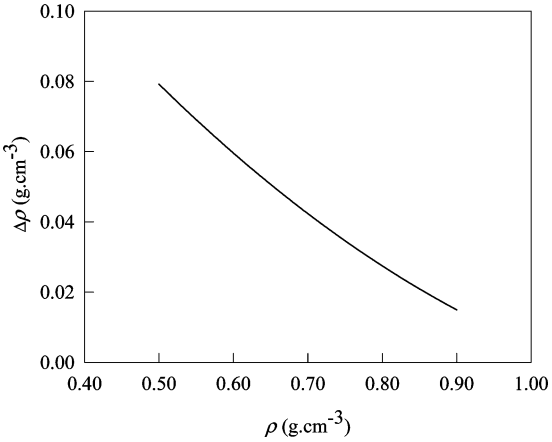

Figure 9. Local solvent density excess for $Fe(Cp^*)_2PF_6$ in supercritical CHF_3 at 323.15 K.

TABLE 5: Values of D_1/D_2, Calculated from eq 17

density, ρ (g/cm^3)	D_1/D_2
0.85	0.38
0.65	1.06
dichloromethane	1.61

on a single ion of radius $R = 0.574$ nm, then the CC model predicts diffusion coefficients that, at low densities ($\rho < 0.8$ g/cm^3), are much smaller than the experimental values, as shown in Figure 7. Note that we used the simple version of the CC model, as in the accompanying paper,[26] without the electroviscous effect, because of the lack of information on Debye relaxation time for the solvent.

Clearly, the assumption that the solvent electrostriction on the ion pair is similar to that of an ion whose size is equivalent to that of the ion pair underestimates the diffusion of the ion pair. The ion-pair electrostriction could be calculated using an extended CC model that was developed by Luo and Tucker,[55] which accounts for clustering in complexes that have a known charge distribution. Unfortunately, the charge distribution in the $Fe(Cp^*)_2PF_6$ ion pair is not easy to estimate, and, consequently, we only may speculate that the electrostriction on this large ion pair would be much lower than that on a single charged ion of equivalent size.

It is possible to gain insight on the diffusion coefficient D_1 of the $Fe(Cp^*)_2^+$ ion by resorting to the I_L value measured at $c_S \rightarrow 0$ (more precisely, SR = 0.01) reported in Table 2. In this case, eq 10 is valid and can be rewritten as

$$I^* = 1 - f(\beta_2) + \frac{D_1}{D_3}\left(1 - f(\beta_2) + 2\frac{D_1}{D_2}f(\beta_2)\right) \qquad (18)$$

where

$$f(\beta_2) = \frac{(1 + 4\beta_2 c_E)^{1/2} - 1}{2\beta_2 c_E} \qquad (19)$$

Because β_2 and D_2 are known, D_1 can be calculated if a reasonable assumption is made in regard to the value of D_3, which is the diffusion coefficient of PF_6^- in supercritical CHF_3. For instance, one can assume that the ratio D_1/D_3 in supercritical CHF_3 is equal to the ratio of the molar conductivities at infinite dilution of $Fe(Cp^*)_2^+$ and PF_6^- ions in organic solvents of similar dielectric constant;[56] that is, $D_1/D_3 \approx 0.56$.

The calculated values of D_1/D_2 are listed in Table 5. At a density of $\rho = 0.85$ g/cm^3, the diffusion coefficient of the $Fe(Cp^*)_2^+$ ion is lower than that of the ion pair, as expected for

the solvation of a charged species, compared to a polar ion pair, in a dense solvent. However, at $\rho = 0.65$ g/cm^3, the diffusion coefficients become similar, which is consistent with the view of a high local density around the ion and the ion pair at low density, which, in turn, generates solvated species of large effective size and, consequently, similar diffusion coefficients. In dichloromethane,[28] the value of D_1 is greater than that of D_2, because the solvation effect is probably negligible and the diffusion coefficient is determined by the solute size.

The estimated values of D_1 at $\rho = 0.85$ and 0.65 g/cm^3 are 3×10^{-5} and 1×10^{-4} cm^2/s, respectively. The CC model, on the other hand, predicts D_1 values of 8×10^{-5} cm^2/s at $\rho = 0.85$ g/cm^3 and 9×10^{-5} cm^2/s at $\rho = 0.65$ g/cm^3, if the radius of the $Fe(Cp^*)_2^+$ ion is assumed to be 0.409 nm.[26] Taking into account that the observed differences between calculated and experimental limiting conductivities for $Fe(Cp^*)_2PF_6$, as a function of density (see Figure 5 in the accompanying paper[26]) show opposite effects (that is, the CC model predicts a much-higher conductivity at low density), we concluded that the assumption of $D_1/D_3 \approx 0.56$ is not valid in supercritical CHF_3 or the lack of an electroviscous term in the simple CC model affects the diffusion and conductivity processes in different ways.

Conclusions

The voltammetric limiting currents for the reduction of the decamethylferrocenium ion ($Fe(Cp^*)_2^+$) and the oxidation of decamethylferrocene ($Fe(Cp^*)_2$) in supercritical and subcritical trifluoromethane (CHF_3) with tetrabutylammonium hexafluorophosphate ($TBAPF_6$) as the supporting electrolyte were measured in a high-pressure electrochemical cell with a platinum disk microelectrode, as a function of temperature and density. The diffusion coefficients of the different species in solution were determined from the limiting currents by resorting to the Oldham, Cardwell, Santos, and Bond (OCSB) theory and using the ion-pair formation constants measured previously by a conductometric technique.

The results were analyzed on the basis of the Stokes−Einstein (SE) model that was valid in the continuum hydrodynamic limit. Although the continuum model is valid all over the entire density range for the neutral $Fe(Cp^*)_2$, the diffusion coefficient for the $Fe(Cp^*)_2PF_6$ ion pair has been observed to deviate from the SE predictions. This behavior is consistent with that observed in the study of the limiting molar conductivity of the $Fe(Cp^*)_2^+$ ion, and it can be explained by assuming that, in the low-density regime ($\rho < 0.7$ g/cm^3), the local density increment that is due to the clustering of solvent molecules on the polar solute results in an increase of the effective radius of the diffusing species.

The CC model, as known for solvent electrostriction on ions, predicts a reduction of the ion-pair diffusion that is much greater than that observed experimentally.

Acknowledgment. Work performed as part of CNEA-CAC-UAQ Project 99-Q-01-07. Financial support from CONICET (PID 384/98) is greatly appreciated. H.R.C. is a member of Carrera del Investigador Científico del Consejo Nacional de Investigaciones Científicas y Técnicas (CONICET). D.L.G. thanks CNEA for a graduate fellowship.

References and Notes

(1) Cooper, A. I. *J. Mater. Chem.* **2000**, *10*, 207.
(2) Kendall, J. L.; Canelas, D. A.; Young, J. L.; DeSimone, J. M. *Chem. Rev.* **1999**, *99*, 543.
(3) McHugh, M. A.; Krukonis, V. J. *Supercritical Fluid Extraction*, 2nd ed.; Butterworth−Heinemann: Stoneham, MA, 1994.
(4) Suárez, J. J.; Medina, I.; Bueno, J. L. *Fluid Phase Equilib.* **1998**, *153*, 167.
(5) He, C. *Fluid Phase Equilib.* **1998**, *147*, 309.
(6) Dinjus, E.; Fornika, R.; Scholz, M. *Chemistry Under Extreme or Non-Classical Conditions*; van Eldik, R., Hubbard, C. D., Eds.; Wiley−Interscience: New York, 1996; Chapter 6.
(7) Silvestri, G.; Gambino, S.; Filardo, G.; Cuccia, C.; Guarino, E. *Angew. Chem.* **1981**, *93*, 131.
(8) Abbott, A. P.; Harper, J. C. *J. Chem. Soc., Faraday Trans.* **1996**, *92*, 3895.
(9) Crooks, R. M.; Bard, A. J. *J. Electroanal. Chem.* **1988**, *240*, 253.
(10) Crooks, R. M.; Bard, A. J. *J. Phys. Chem.* **1987**, *91*, 1274.
(11) Crooks, R. R.; Fan, F.-R. F.; Bard, A. J. *J. Am. Chem. Soc.* **1984**, *106*, 6851.
(12) Cabrera, C. R.; García, E.; Bard, A. J. *J. Electroanal. Chem.* **1989**, *260*, 457.
(13) Crooks, R. M.; Bard, A. J. *J. Electroanal. Chem.* **1988**, *243*, 117.
(14) Cabrera, C. R.; Bard, A. J. *J. Electroanal. Chem.* **1989**, *273*, 147.
(15) Liu, C.-Y.; Snyder, S. R.; Bard, A. J. *J. Phys. Chem. B* **1997**, *101*, 1180.
(16) Bard, A. J.; Flarsheim, W. M.; Johnston, K. P. *J. Electrochem. Soc.* **1988**, *135*, 1939.
(17) McDonald, A. C.; Fan, F.-R. F.; Bard, A. J. *J. Phys. Chem.* **1986**, *90*, 196.
(18) Flarsheim, W. M.; Tsou, Y.-M.; Trachtemberg, I.; Johnston, K. P.; Bard, A. J. *J. Phys. Chem.* **1986**, *90*, 3934.
(19) Philips, M. E.; Deakin, M. R.; Novotny, M. V.; Wightman, R. M. *J. Phys. Chem.* **1987**, *91*, 3934.
(20) Niehaus, D.; Philips, M.; Michael, A.; Wightman, R. M. *J. Phys. Chem.* **1989**, *93*, 6232.
(21) Olsen, S.; Tallman, D. E. *Anal. Chem.* **1994**, *66*, 503.
(22) Olsen, S.; Tallman, D. E. *Anal. Chem.* **1996**, *68*, 2054.
(23) Abbott, A. P.; Eardley, C. A.; Harper, J. C. *J. Electroanal. Chem.* **1998**, *457*, 1.
(24) Abbott, A. P.; Eardley, C. A. *J. Phys. Chem. B* **2000**, *104*, 775.
(25) Abbott, A. P.; Eardley, C. A. *J. Phys. Chem. B* **2000**, *104*, 9351.
(26) Goldfarb, D. L.; Corti, H. R. *J. Phys. Chem. B* **2004**, *108*, 3358−3367.
(27) Xiao, C.; Wood, R. H. *J. Phys. Chem. B* **2000**, *104*, 918.
(28) Goldfarb, D. L.; Corti, H. R. *Electrochem. Commun.* **2000**, *2*, 663.
(29) Duggan, D. M.; Hendrickson, D. N. *Inorg. Chem.* **1975**, *14*, 955.
(30) Amatore, C.; Deakin, M. R.; Wightman, R. *J. Electroanal. Chem.* **1987**, *220*, 49.
(31) Oldham, K. B. *J. Electroanal. Chem.* **1988**, *250*, 1.
(32) Aoki, K. *Electroanalysis* **1993**, *5*, 627.
(33) Bond, A. M.; Oldham, K. B.; Zoski, C. G. *Anal. Chim. Acta* **1989**, *216*, 177.
(34) Cooper, J. B.; Bond, A. M. *J. Electroanal. Chem.* **1991**, *315*, 143.
(35) Cooper, J. B.; Bond, A. M. *J. Electroanal. Chem.* **1992**, *331*, 877.
(36) Oldham, K. B.; Cardwell, T. J.; Santos, J. H.; Bond, A. M. *J. Electroanal. Chem.* **1997**, *430*, 25.
(37) Goldfarb, D. L.; Corti, H. R. *J. Electroanal. Chem.* **2001**, *509*, 155.
(38) Oldham, K. B.; Cardwell, T. J.; Santos, J. H.; Bond, A. M. *J. Electroanal. Chem.* **1997**, *430*, 39.
(39) Rubio, R. G.; Zollweg, J. A.; Street, W. B. *Ber. Bunsen−Ges.* **1989**, *93*, 791.
(40) Altunin, V. V.; Geller, V. Z.; Petrov, E. K.; Rsskazov, D. C.; Spiridinov, G. A. *Thermophysical Properties of Freons*; Selover, T. B., Jr., Ed.; Methane Series, Part 1; Hemisphere Publishing Co.: Washington, DC, 1987.
(41) Reuter, K.; Rosenzweig, S.; Franck, E. U. *Physica A* **1989**, *156*, 294.
(42) Silva, S. M.; Macedo, E. *Ind. Eng. Chem. Res.* **1998**, *37*, 1490.
(43) Swaid, I.; Schneider, G. M. *Ber. Bunsen−Ges.* **1979**, *83*, 969.
(44) Funazukuri, T.; Nishimoto, N. *Fluid Phase Equilib.* **1996**, *125*, 235.
(45) Lamb, D.; Adamy, S. T.; Woo, K. W. *J. Phys. Chem.* **1989**, *93*, 5002.
(46) Feist, R.; Schneider, G. M. *Sep. Sci. Technol.* **1982**, *17*, 261.
(47) Hayduk, W.; Cheng, S. C. *Chem. Eng. Sci.* **1971**, *26*, 635.
(48) Debenedetti, P. G.; Reid, R. C. *AIChE J.* **1986**, *32*, 2034.
(49) Funazukuri, T.; Ishiwata, Y.; Wakao, N. *AIChE J.* **1992**, *38*, 1761.
(50) Marken, F.; Goldfarb, D. L.; Compton, R. G. *Electroanalysis* **1998**, *10*, 562.
(51) Kanda, D.; Kimura, Y.; Terazima, M.; Hirota, N. *Ber. Bunsen−Ges.* **1997**, *101*, 4442.
(52) Heitz, M. P.; Maroncelli, M. *J. Phys. Chem. A* **1997**, *101*, 5852.
(53) Wada, N.; Saito, M.; Kitada, D.; Smith, R. L., Jr.; Inomata, H.; Arai, K.; Saito, S. *J. Phys. Chem. B* **1997**, *101*, 10918.
(54) Fernández-Prini, R.; Japas, M. L. *Chem. Soc. Rev.* **1994**, *23*, 155.
(55) Luo, H.; Tucker, S. C. *J. Phys. Chem.* **1997**, *101*, 1063.
(56) Goldfarb, D. L.; Longinotti, M. P.; Corti, H. R. *J. Solution Chem.* **2001**, *30*, 307.